Implementation of a staggered trigger algorithm by velocity difference dealiasing rules

Fábio Rizental Coutinho[1]

[1] Department of Electronic Engineering, Federal University of Technology-Paraná (UTFPR) Campus Toledo-PR 85902-490 Brazil

The staggered trigger technique consists of alternating between a long and a short Pulse Repetition Time (PRT) to mitigate the range-velocity ambiguity. Due to the two PRT, two different velocities can be estimated. The difference of these two velocities can be used to determine in which Nyquist interval is the real flow velocity. This method was originally proposed for Doppler weather radar where velocity folding factors are restricted to 2 times the conventional maximum velocity of the short PRT. In this work the staggered trigger method using the velocity difference for dealiasing purpose is further extended to a higher velocity folding factor. We show that emitting a 4-cycle ultrasound pulse this method can reach up to 5 times the conventional maximum velocity of the long PRT. The algorithm was tested using ultrasound simulation software - Field II. The simulation consisted of a piston transducer emitting in a flow with a uniform velocity profile. The performance of the technique was also evaluated on several low SNR conditions.

Keywords: staggered trigger, dealiasing, velocity aliasing, ultrasound velocity profiling.

1. Introduction

Ultrasonic Doppler velocity profiler (UVP) is a fundamental technique for research in fluid engineering filed [1]. The method estimates the velocity along the measurement line by using periodic short bursts of ultrasound. However this pulsed strategy limits the maximum range that can be measured. Increasing the time period between bursts can extend the measurement range but comes with a proportional reduction in the maximum velocity that can be measured. If the real velocity is higher than the maximum velocity allowed then velocity aliasing will occur [2]. The velocity aliasing problem can be overcome by dealiasing techniques. Insonating the flow using two transducers with different frequencies is a method that can resolve velocity aliasing problem. This method, also called multi-frequency has been proposed by [3-5]. In this technique the information of the velocity from each transducer are combined in such a way that the whole system can be viewed as one, whose frequency is the difference between the two transducers frequencies. Another technique to avoid alias is the velocity-matched spectrum analysis [6]. In this approach the data from each pulse emission are arranged in a two dimensional matrix. A velocity spectrum is obtained by analyzing the shift in each pulse emission through iso-velocity lines [6]. Since the method results in a spectrum of velocities, this technique is computational intensive. Wide band or time-shift estimation techniques such as cross-correlation [7] do not suffer from aliasing under a high SNR condition. However cross-correlation algorithms usually are more time consuming that the conventional autocorrelation algorithm. Extend autocorrelation technique [8] combines phase-shift estimation with cross-correlation. The combination can reduce significantly the amount of computation. However, the processing time of this approach is still very high (approximately 55 times slower) than the autocorrelation algorithm [9]. Staggered trigger or staggered PRT (Pulse Repetition Time) is characterized by using a non-uniform pulse repetition time. Staggered trigger alternate the pulse emission with a long and a short PRT. Contrasting to multi-frequency, staggered PRT only needs one transducer. And the processing time is comparable with the autocorrelation. This technique was first introduced for blood flow measurement [10]. Later, it was also further extended for weather radar field [11-12]. Recently, Murakawa et al [13] adapted it to fluid engineering, implementing a higher flowrate measurement system. They reported that the velocity error of the practical system was too high to measure velocity directly. Thus they used the staggered PRT velocity only to discover the number of aliasing or aliasing factor. However, this strategy still was not enough to deliver an accurate velocity profile. Therefore, they have used a moving average filter and relaxed the velocity time resolution. The measurement configuration used a high number of pulse (N_{pulse}=512) for every velocity estimate, and velocity profile was obtained through averaging 1,000 instantaneous velocity profiles. They reported an error of -0.8% and maximum measured velocity of 6 times larger than the conventional UVP method [13]. Torres and Dubel [14] proposed a new algorithm for staggered trigger that uses the velocity difference from the velocities estimated by the long and short PRT to decide the velocity dealiasing factor. Their work was focused in weather radar and they showed that their method could measure velocity up to 3 times greater than the maximum conventional velocity regarding the long PRT. In this work we adapted the methodology of [14] for fluid engineering. It is also showed that the method proposed can reach even higher velocities than described in [14]. The algorithm was implemented and tested using an ultrasound simulator. The result shows that it is possible to measure velocity up to 5 times higher than the conventional velocity regarding the long PRT. Also this technique does not need intensive averaging or high N_{pulse}. The results are also tested under low SNR simulated condition.

2. Staggered trigger by velocity difference method

2.1 Foundation of staggered trigger method

In staggered trigger, an ultrasonic pulsed wave is emitted in alternating time intervals, T_1 and T_2, with $T_2 > T_1$. Velocity estimation is evaluated by the lag one autocorrelation algorithm [7] using only adjacent pulses whose time interval is equal. So the velocity relative to T_1, v_1, and the velocity relative to T_2, v_2, can be estimated using the following relations

$$v_1 = \frac{c}{4\pi f T_1}\arg\big(R(T_1)\big), \qquad (1)$$

$$v_2 = \frac{c}{4\pi f T_2}\arg\big(R(T_2)\big), \qquad (2)$$

respectively, where c denotes the sound velocity in the considered medium, f represents the transducer central frequency, arg is the principal argument restricted to the range (-π,π] and $R(\cdot)$ is the autocorrelation function. The maximum measured velocity is determined by the range of the principal argument as

$$v_{a1} = \frac{c}{4fT_1}, \qquad (3)$$

$$v_{a2} = \frac{c}{4fT_2}. \qquad (4)$$

Staggered trigger method combines each lag one autocorrelation to result in a dealiased velocity estimated by

$$v_{st} = \frac{c}{4\pi f(T_2 - T_1)}\Big(\arg\big(R(T_1)\big) - \arg\big(R(T_2)\big)\Big). \qquad (5)$$

And the staggered trigger maximum velocity will be

$$v_{max,st} = \frac{c}{4f(T_2 - T_1)}, \qquad (6)$$

which will be higher than Eqs. (3) and (4) if $T_2 - T_1$ were small relatively to T_1 or T_2. However, velocity estimated using Eq. (5) will have a high uncertainty for some velocity intervals. Because of this Eq. (5) is not used in practical implementation. Therefore, to measure velocity above Nyquist limit, Eqs. (1) and (2) are combined with some rule to discover the velocity aliasing factor.

2.2 Velocity difference dealiasing rules

The $v_1 - v_2$ velocity difference can be used to determine the aliasing factor of v_1 or v_2 if the ratio $T_1/T_2 = m/n$, follow the condition that m and n should be relatively prime integers [14]. Applying this ratio, the maximum unambiguous velocity that can be measure are $v_{ua1} = mv_{a1}$ and $v_{ua2} = nv_{a2}$, for v_1 and v_2, respectively. The velocity difference rule can be demonstrated graphically. The velocity aliasing incurs that v_1 or v_2 cannot be higher than $\pm v_{a1}$ or $\pm v_{a2}$, respectively. By plotting the real velocity versus $v_1 - v_2$ the graph of Fig. 1 is obtained, for $m/n = 3/4$. Note in Fig.1, that, when v_1 is aliased, or $v_{a1} < v_1 < 3v_{a1}$, the velocity difference assumes two unique constant values ($-0.5v_{a1}$ and $+v_{a1}$). A similar behavior happens to negative aliasing in v_1, or the condition that $-3v_{a1} < v_1 < -v_{a1}$, in this case $v_1 - v_2$ assumes $+0.5v_{a1}$ and $-v_{a1}$. In the case of aliasing in v_2, one can notice (Fig.1) that for the first aliasing, i.e. when $v_{a2} < v_2 < 3v_{a2}$ (or $-3v_{a2} < v_2 < -v_{a2}$ for negative aliasing) the velocity difference assumes $2v_{a2}$ and $-0.5v_{a1}$ (or $-2v_{a2}$ and $+0.5v_{a1}$ for negative aliasing). When v_2 aliases for the second time, i.e. when $v_2 > 3v_{a2}$ (or $v_2 < -3v_{a2}$ for negative aliasing) then $v_1 - v_2$ equals to v_{a1} (or $-v_{a1}$ for negative aliasing). Therefore, $v_1 - v_2$ maps the aliasing factor in v_1 or v_2. In [14] it is show that this function bijection occurs for any m/n, if m and n are relatively prime integers. However, they mention that in practical implementation only $m/n = 2/3$ showed good results.

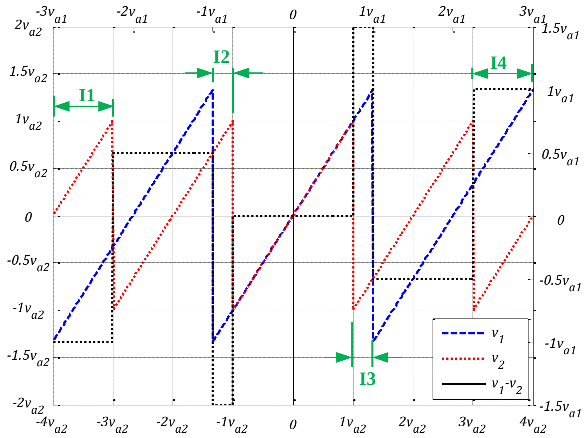

Figure 1: Velocity difference ($v_1 - v_2$) and aliased velocities v_1 and v_2 as a function of the real Doppler velocity. Time interval ratio used was $T_1/T_2 = m/n = 3/4$.

3. Simulation procedure

The algorithm was tested using Field II (release 3.24) simulation software running under Matlab R2013a environment. Field II uses linear system theory to evaluate the pulsed ultrasound field as a function of time at a specific point in space [15-16]. Simulations were carried at a 100 MHz sampling frequency. The transducer simulated was a piston shaped transducer with 10 mm diameter. Transducer geometry was divided into 1.2 mm x 1.2 mm square mathematical elements (Fig. 2). Since the real transducer edges might vibrate less than the center, apodization coefficients were defined based in a 2D hanning mask (Fig. 2). Ultrasound central frequency was 4 MHz and transducer excitation was performed by a 4-cycle sinusoidal burst. The flow was simulated in a section of 30 mm ID pipe (Fig. 3). Transducer was positioned 25 mm from pipe and at an angle of 45 degrees with respect to the z axis (Fig. 3). The number of reflectors was set-up to 10 scatterers per measurement volume. Pipe wall thickness was defined as 2 mm. The amplitude from moving reflectors was configured to be 100 times greater than the amplitude of echoes from pipe wall. This configuration was used to avoid using clutter filters that could introduce bias in the results. Sound velocity in the flow was set-up to 1480 m/s. A flow with uniform velocity profile was simulated. Five combinations of PRTs were tested. Short PRT was fixed in $T_1 = 0.5$ ms and a set of long PRT were tested: $T_2 = \{0.667, 0.571, 0.625, 0.6, 0.583, 0.571\}$ ms which gives the following PRT ratios $T_1/T_2 = m/n = \{3/4, 4/5, 5/6, 6/7, 7/8\}$, respectively. Flow velocities simulated were based in multiples of the maximum conventional velocity of the short PRT, v_{a1}. The maximum dealiased velocities that can be measured by the proposed algorithm are $3v_{a1}, 4v_{a1}, 5v_{a1}, 6v_{a1}$ and $7v_{a1}$, for $m/n = 3/4, 4/5, 5/6, 6/7$ and $7/8$, respectively.

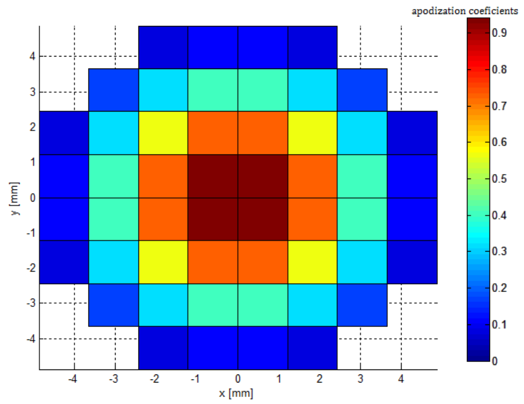

Figure 2: Display of the geometry and apodization of the piston shaped transducer simulated.

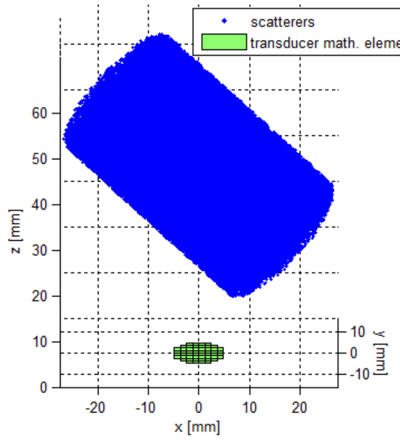

Figure 3: 3D graph of scatterers distribution with respect to the ultrasound transducer (x-y plane). Pipe walls were suppressed.

Therefore velocities from $0.5v_{a1}$ up to maximum dealiased were tested for each case. For each flow, a total of 2000 ultrasound emissions were simulated which give roughly 1 second of acquired data. To evaluate the performance of the algorithm under real conditions, signal-to-noise ratio from 50 dB to 0 dB were performed. Velocity estimation was carried by an autocorrelation algorithm followed by applying the velocity difference dealiasing rules algorithm. The number of pulses used to estimate the velocity was N_{pulse}=50. To calculate the velocity profile, 40 instantaneous profiles were averaged for N_{pulse}=50. Velocity profiles were obtained using raw estimated velocities, i.e., without any kind of velocity post-processing techniques.

4. Results

Mean spatial velocity profile estimation was evaluated using Eq. 5 for each PRT ratio. The error became very high at the vicinities of $1v_{a1}, 3v_{a1}, 5v_{a1}$ regarding the PRT ratio (Fig. 4). This problem occurs whenever v_2 is aliased but v_1 is still non aliased (Fig. 1 intervals: I1, I2, I3 and I4). In this condition $\arg(R(T_2))$ of Eq. 5 is negative while $\arg(R(T_1))$is positive which will result in an erroneous velocity estimate using Eq. 5. Because of this large error, Eq. 5 is usually not used.

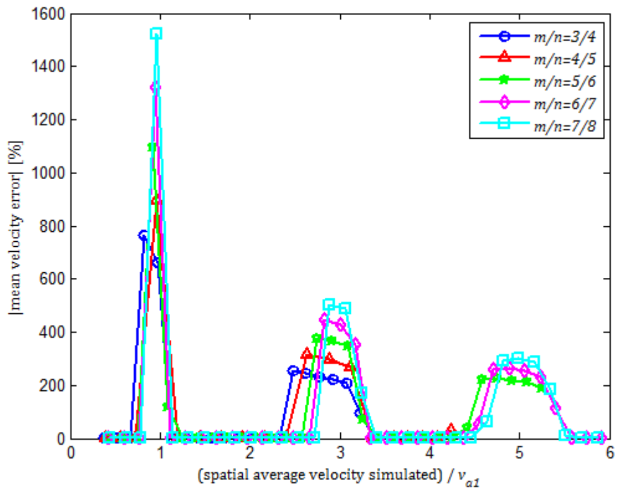

Figure 4: Mean spatial velocity profile relative error evaluated using Eq. 5.

To verify the maximum PRT ratio that can be used in the aforementioned simulated conditions, the mean spatial velocity simulated versus the mean spatial velocity measured plot were evaluated for each PRT ratio (Fig. 5).

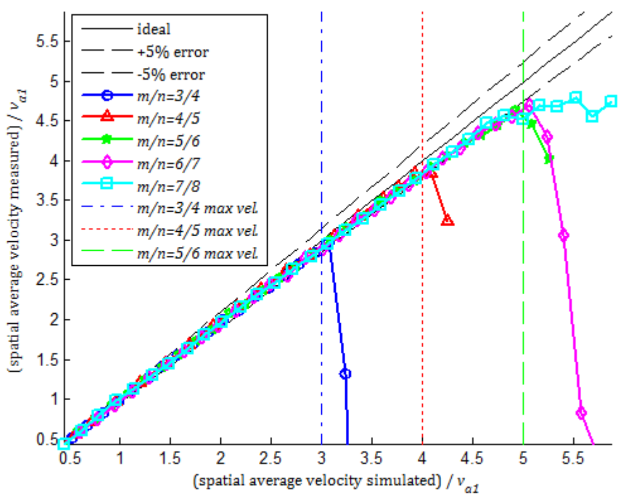

Figure 5: Spatial averaged velocity simulated versus spatial average velocity measured (normalized by conventional maximum velocity relatively to T1) for SNR=30 dB, N_{pulse}=50.

Velocity was estimated under a SNR=30 dB. Velocities were normalized by the maximum conventional velocity regarding T_1, v_{a1}. Note that for PRT ratios: 3/4, 4/5 and 5/6 the mean velocity measured deviates abruptly from the 5% error line after surpassing the maximum dealiased velocity regarding each ratio (Fig. 5). However, PRT ratios 6/7 and 7/8 deviate earlier than expected (theoretically maximum dealiased velocity should be

$6v_{a1}$ and $7v_{a1}$, respectively) at $5v_{a1}$. It should be noted that as the mean simulated velocity increases (for values under the maximum dealiased velocity) the mean spatial velocity begins to be underestimated. Such behavior may be improved by the use of post-processing techniques or increasing the N_{pulse}.

Velocity profile reproducibility was assessed using the mean squared error, MSE, of the velocity profile for PRT ratios from 3/4, 4/5 to 5/6 (Fig. 6). Performances under different SNR conditions, from 20 dB to 0 dB were evaluated. Spatial velocity profile estimation becomes worse for velocities above Nyquist limit (when (spatial average velocity simulated)/ $v_{a1} \geq 1$). This behavior occurs mainly under low SNR conditions. It is expected that the error increases with velocity because the variance of the velocity estimate increases due to intrinsic spectral broadening. The MSE climbs up for flow velocities higher than $3v_{a1}, 4v_{a1}$ and $5v_{a1}$ in Fig. 6, respectively, regarding the SNR condition. This result agrees with the maximum dealiased velocity that can be measured in each case. Profile reproducibility also becomes worse when having simultaneously low SNR condition (10-0 dB) and low PRT ratio (Fig. 6c). Depending on the accuracy needed, this condition can limit the maximum dealiased velocity to a lower value.

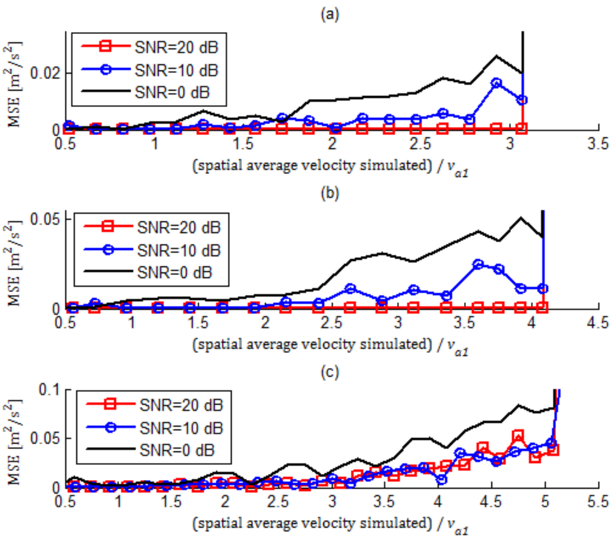

Figure 6: Velocity profile mean squared error for (N_{pulse}=50): (a) $m/n = 3/4$, (b) $m/n = 4/5$, and (c) $m/n = 5/6$.

5. Conclusions

The algorithm for staggered trigger by using velocity difference dealiasing rules originally proposed by [14] was adapted to fluid engineering application. It was showed that the implementation of [14] can be further extended to PRT ratios lower than $m/n = 2/3$ thus allowing measurement of higher velocities than the conventional. Simulation results shown that using a 4 Mhz transducer with 4-cycle sinusoidal burst excitation and a low PRT of 0.5 ms the maximum pratical PRT ratio is $m/n = 5/6$. In this condition it is possible to measure velocities up to 5 times the Nyquist limit. However, using a lowest possible PRT($m/n = 5/6$) is only feasible at relatively high SNR conditions. Under low SNR, PRT ratios of 4/5 and 3/4 should perform better regarding the reproducibility of the velocity profile. We believe that the reason for the proposed implementation to reach lower PRT ratio than the one described in [14] is because of the 4-cycle excitation versus the 1-cycle excitation used in WSR-88D weather radars. Experimental tests should be conducted to confirm the simulated results in a future work. Also, relationship between transducer frequency, excitation, etc with maximum dealiased velocity that can be measured should be investigated.

6. Acknowledgments

This work was carried out with the support of Fundação Araucária (grant 06A/2014) and Secretaria de Estado da Ciência, Tecnologia e Ensino Superior do Paraná (SETI).

References

[1] Takeda Y: Velocity profile measurement by ultrasonic Doppler method, Exp. Fluids, 10 (1995), 444-453.
[2] Takeda Y: Ultrasonic Doppler fluid flow, Springer, Japan (2012).
[3] Fer R, *et al.*: New Advances in colour flow mapping: quantitative velocity measurement beyond Nyquist limit. Br J Radio 64 (1991), 651.
[4] Nitzpon HJ, *et al.*: A new pulsed wave Doppler ultrasound system to measure blod velocities beyond Niquist limit. IEEE Trans Ultrason. Ferrroelec. Freq. Contr. 42 (1995), 265-279.
[5] Zedel L & Hay AE: Design and performance of a new Multi-frequency coherent Doppler profiler. 33rd IAHR Congress, 2009.
[6] Torp H & Kristoffersen K: Velocity matched spectrum analysis: a new method for suppressing velocity ambiguity in pulsed-wave Doppler. Ultrasound Med. Biol. 21(1995), 937-944.
[7] Jensen, JA: Estimation of blood velocities using ultrasound: A signal processing approach. Cambridge. University Press, New York, (2006).
[8] Lai X & Torp H: An Extended Autocorrelation Method for Estimation of Blood Velocity, IEEE Trans. Ultrason., Ferroelec., Freq. Contr. 44 (2007), 1332-1342.
[9] Ofuchi, CY, *et al.*: Extended autocorrelation velocity estimator applied to fluid engineering, Proc. of the 9th ISUD, Strasbourg (2014), 109-112.
[10] Nishiyama H & Katakura K. Non-equally-spaced pulse transmission for non-aliasing ultrasonic pulsed Doppler measurement, J. Acoust. Soc. Jpn. 13, 4 (1992), 215-222.
[11] Franca MJ & Lemmin U: Eliminating velocity aliasing in acoustic Doppler velocity profiler data, Meas. Sci. Tech. 17 (2006), 313-322.
[12] Holleman I & Beekhuis H: Analysis and Correction of Dual PRF Velocity Data, J. Atmos. Ocean. Technol. 20 (2003), 443-453.
[13] Murakawa H, *et al.*: Higher flowrate measurement using ultrasonic pulsed Doppler method with staggered trigger. Proc. of the 9th ISUD, Strasbourg (2014), 117-120.
[14] Torres SM & Dubel Y: Design, implementation, and demonstration of a staggered PRT algorithm for the WSR-88D. J. Atmos. Oceanic Tech. 21 (2004), 1389-1399.
[15] Jensen JA & Svendsen NB: Calculation of pressure fields from arbitrarily shaped, apodized, and excited ultrasound transducers. IEEE Trans. Ultrason., Ferroelec., Freq. Contr. 39(1992), 262-267.
[16] Jensen JA: A program for simulating ultrasound systems. Med. Biol. Eng. Comp., 10th Nordic-Baltic Conf. on Biom. Imag., Vol.4, Supplement 1, Part1 (1996b), 351–353.